Materials Physics and Mechanics 41 (2019) 19-29 Received: January 31, 2018

LEAKAGE CURRENT IN AlGaN SCHOTTKY DIODE IN TERMS OF THE PHONON-ASSISTED TUNNELING MODEL

V.S. Volcheck*, V.R. Stempitsky

Department of Micro- and Nanoelectronics, Belarusian State University of Informatics and Radioelectronics

P. Brovka 6, 220013, Minsk, Belarus

*e-mail: vlad.volchek@bsuir.by

Abstract. The leakage current in the AlGaN Schottky diode under a reverse bias is simulated and compared within the frameworks of the thermionic emission–diffusion and phonon-assisted tunneling models. It is shown that the phonon-assisted tunneling model is suitable to describe the reverse-bias characteristic of the AlGaN Schottky contact and can also be applied to calculate the gate leakage current in the AlGaN/GaN high electron mobility transistor.
Keywords: electron tunneling, leakage current, Schottky diode, thermionic emission

1. Introduction

In recent decades, GaN has constantly attracted interest of material researchers and device engineers due to its specific properties afforded by its wide band gap. The AlGaN/GaN high electron mobility transistor (HEMT) has been regarded as a leading candidate for high power microwave applications since its invention in 1993. Nevertheless, in spite of all scientific and technological advances, nitride-based electronics still faces big challenges hindering its commercial viability. One of the critical disadvantages of HEMTs, especially Schottky-barrier transistors, is an abnormal reverse-bias leakage current through the gate, which dramatically degrades device performance and reliability. The common approach to the problem is based on the insertion of dielectric materials with high permittivity into the gate structure [1,2]. Although this technique proves to be very effective in suppressing the leakage current, the issue is yet to be tackled, since the proposed solutions remain complex and expensive.

Until now, investigators have put forward different suggestions about mechanisms of the reverse-bias leakage current in rectifying contacts to GaN and AlGaN. For instance, in Ref. [3], two dominant leakage current mechanisms in the Ni/n-GaN Schottky diode structure grown by molecular-beam epitaxy were identified; one being associated with field emission tunneling and another with an exponential temperature dependence consistent with either trap-assisted tunneling or one-dimensional hopping conduction. In Ref. [4], temperature dependencies of the reverse-bias leakage current in rectifying contacts to both n-GaN and $Al_{0.25}Ga_{0.75}N$/GaN epitaxial layer structures were obtained; it is revealed that the tunneling current is dominant at temperatures below 150 K, while Frenkel-Poole emission controls the current at temperatures above 250 K. The study of electrical behavior of Au/Ni/GaN Schottky diodes in a temperature range of 300 to 623 K revealed that the current-voltage characteristics are described by a thermionic emission model with a Gaussian distribution of barrier heights at temperatures below 503 K, whereas the leakage current is governed by the generation-recombination process at higher temperatures [5]. It was supposed [6] that Frenkel-Poole emission is responsible for the reverse-bias carrier transport in Schottky diodes fabricated on $Al_{0.83}In_{0.17}N$/AlN/GaN heterostructures in a temperature range of 250 to 375 K. The authors

http://dx.doi.org/10.18720/MPM.4112019_4
© 2019, Peter the Great St. Petersburg Polytechnic University
© 2019, Institute of Problems of Mechanical Engineering RAS

of Ref. [7] demonstrated that one of the dominant leakage current mechanisms in the Ni/GaN Schottky sample annealed at 1423 K for 5 minutes was one-dimensional hopping conduction.

A variety of proposed conduction mechanisms employed to estimate the reverse-bias leakage current in GaN Schottky diodes means that fundamental properties of the carrier transport in rectifying contacts to GaN have not yet been completely understood. However, it is claimed in Ref. [8] that the reverse-bias leakage current in the Ni/n-GaN Schottky diode can be interpreted in terms of the phonon-assisted tunneling (PAT) model. Although it is contemplated specially for GaN, the model should remain valid for associated compounds, such as AlGaN [9], thus enabling to accurately describe the transfer characteristic of the AlGaN/GaN Schottky-barrier HEMT.

In this communication, we would like to explain the peculiarities of the reverse-bias leakage current in the AlGaN Schottky diode within the framework of the PAT model, since this device can essentially be treated as an equivalent to the gate junction in the conventional AlGaN/GaN HEMT.

2. Simulation Details

In order to investigate the application of the PAT model to AlGaN, Ni/AlGaN Schottky diode structures were simulated within the framework of the thermionic emission–diffusion (TED) theory [10] and expanded by incorporating the PAT model.

Device structure. The two-dimensional device structure consists of an $Al_{0.3}Ga_{0.7}N$ region occupying the entire simulation domain with a length of 1 μm and a variable width denoted by w. Imposed boundary conditions for the primary equations define the electrodes of the Schottky diode. A rectangular mesh consisting of a series of lines along x- and y-directions is constructed to represent the simulation domain. The distance between the mesh lines perpendicular to the anode and the cathode $\Delta x = 5\cdot 10^{-5}$ cm, while the lines parallel to the electrodes are located with a spacing $\Delta y = 10^{-8}$ cm. The significantly finer mesh along the y-direction is vital, since it allows the space-charge region to be accurately simulated.

Thermionic emission–diffusion model. The electrical behavior of semiconductor devices is operated by a mathematical model consisting of a coupled set of fundamental partial differential equations, which link together the electrostatic potential and the electron concentration. The primary function of general purpose device simulators is to find a self-consistent solution of these equations ensuring the potential profile inside the simulation domain being consistent with its electron concentration profile. The general framework of the model is provided by the Poisson and current continuity equations. The Poisson equation governs the interaction of the electrostatic potential with the space charge density:

$$\nabla^2\varphi = \frac{q\left(N_d - n\right)}{\varepsilon\varepsilon_0}, \tag{1}$$

where φ is the electrostatic potential, q is the elementary electric charge, N_d is the donor density, n is the electron concentration, ε is the relative permittivity and ε_0 is the electric constant.

In equation (1), the acceptor density and the hole concentration are omitted. From now on, any values associated with the minority carriers are neglected.

The continuity equation describes the way the electron concentration evolves as a result of transport, generation and recombination processes. In a steady state, the generation and recombination rates are equal, the electron concentration is constant, and the continuity equation is given as follows:

$$q\frac{\partial n}{\partial t} = \nabla J = 0, \tag{2}$$

where *J* denotes the electron current density (for simplicity, referred to hereafter as the current).

Two fundamental theories have been proposed to describe the current transport in the Schottky junction. In the space-charge region of the junction, the electron motion is governed by the usual processes of diffusion and drift. When the electrons are transported from the bulk of the semiconductor to the interface, they can be emitted over the top of the barrier into the metal. These two mechanisms are effectively in series and the current is determined predominantly by whichever causes the larger impediment to the flow of electrons. Within the diffusion theory, the first of these two mechanisms is the limiting factor, whereas in accordance with the thermionic emission theory, the second is more important.

The diffusion theory assumes that the electron concentration in the semiconductor immediately adjacent to the interface is independent of the applied bias and the effective recombination velocity is infinite. Since there is a very high concentration of electrons in the metal, the carrier scattering forces the electrons on the semiconductor side of the junction into thermal equilibrium with those in the metal, which is equivalent to saying that the quasi-Fermi level changes throughout the space-charge region and ultimately coincides at the interface with the Fermi level in the metal. In that case, the driving force for conduction electrons is the quasi-Fermi level gradient and the drift-diffusion current takes the form

$$J_{DD} = q\mu n \nabla\varphi_n, \tag{3}$$

where μ is the electron mobility and φ_n is the quasi-Fermi level.

By neglecting the gradient of the intrinsic carrier concentration, which takes into account band gap narrowing effects, the current can be decomposed into drift and diffusion ingredients:

$$J_{DD} = q\mu n E + qD\nabla n, \tag{4}$$

where *D* is the diffusivity and denotes the electric field, which is related to the electrostatic potential through the Gauss law:

$$E = -\nabla\varphi. \tag{5}$$

It should be noted that the derivation of the diffusion model also assumes the validity of the Einstein relation:

$$D = V_T\mu. \tag{6}$$

Here, V_T denotes the thermal voltage:

$$V_T = \frac{\kappa T}{q}, \tag{7}$$

where κ is the Boltzmann constant and *T* is a temperature.

From the thermionic emission theory, the electrons emitted from the semiconductor over the barrier are not in thermal equilibrium with those in the metal and can be treated as "hot" carriers. The hot electrons gradually lose their energy by carrier scattering as they penetrate the metal. As a consequence, the quasi-Fermi level remains flat throughout the space-charge region and does not have to coincide with the metal Fermi level at the interface. The effect of diffusion and drift in the space-charge region are negligible, which, in turn, implies that the electron concentration in the semiconductor nearest to the interface is altered by an exponential factor when a bias is applied and the effective recombination velocity has a certain finite value. The standard formula for the thermionic emission current is given by

$$J_{TE} = AT^2 \exp\left(-\frac{\varphi_b}{V_T}\right)\left[\exp\left(-\frac{\varphi_b}{V_T}\right) - 1\right], \tag{8}$$

where φ_b is the barrier height.

In equation (8), *A* represents the effective Richardson constant:

$$A = \frac{4\pi q \kappa^2 m_{eff} m_e}{h^3}, \tag{9}$$

where m_{eff} is the electron effective mass, m_e is the electron rest mass and h is the Planck constant.

Several researchers have combined the diffusion and thermionic emission models by considering the two mechanisms to be in series and successfully determining the position of the quasi-Fermi level at the interface equalizing the drift-diffusion and thermionic emission currents. The single TED theory developed in Ref. [10] has long been recognized as an appropriate model for describing the current transport in ideal Schottky barrier diodes; the authors introduced the concept of an effective recombination velocity at the top of the barrier (potential energy maximum) and evaluated the current through the metal-semiconductor barrier as follows:

$$J_{TED} = q v_R (n_m - n_{eq}), \tag{10}$$

where v_R is the effective recombination velocity and n_m is the electron concentration at the potential energy maximum when the current is flowing.

In equation (10), n_{eq} is a constant referred to as the "quasi-equilibrium electron concentration" at the potential energy maximum. It means the concentration, which would be obtained if it were possible to reach equilibrium without altering the potential energy maximum. The term with $v_R n_m$ represents the electron flux from the semiconductor to the metal, while the $v_R n_{eq}$ denotes the opposite flux.

The recombination velocity is given by

$$v_R = \frac{AT^2}{qN_c}, \tag{11}$$

where N_c is the effective density of states in the conduction band.

The quasi-equilibrium electron concentration does not depend on the applied bias and is computed in accordance with

$$n_{eq} = N_c \exp\left(-\frac{\varphi_b}{V_T}\right). \tag{12}$$

The actual electron concentration at the top of the barrier is determined by

$$n_m = n_{eq}\left(1 + \frac{v_D}{v_R + v_D}\left[\exp\left(-\frac{\varphi_b}{V_T}\right) - 1\right]\right). \tag{13}$$

Here v_D is the effective diffusion velocity associated with the transport of electrons from the edge of the space-charge region to the potential energy maximum. If the Schottky barrier lowering is comparable to or less than V_T, the effective diffusion velocity is given by

$$v_D = |\mu E|. \tag{14}$$

Inserting equations (12) and (13) into equation (10) yields another formulation of the TED current:

$$J_{TE} = qN_c \frac{v_R v_D}{v_R + v_D} \exp\left(-\frac{\varphi_b}{V_T}\right)\left[\exp\left(-\frac{\varphi_b}{V_T}\right) - 1\right]. \tag{15}$$

If $v_R >> v_D$, the pre-exponential factor in equation (15) is limited by v_D and the current is governed by the processes of diffusion and drift. If, however, $v_R << v_D$, the thermionic emission is dominant. Occasionally, v_R is referred to as the "thermionic emission velocity", which reflects the physical nature of the mechanism [11]. It should be noted that the image-force lowering of the Schottky barrier outlined in Ref. [10] is neglected in equation (15).

Mobility model. For calculating the electron mobility, the low field model [12] is used. It was derived on the basis of fitting a Caughey–Thomas-like model to Monte Carlo

simulation data. The model reflects the influence of temperature and ionized impurity density on the carrier mobility in the binary compounds, InN, GaN and AlN, and their associated ternaries, InGaN, AlGaN and InAlN. When the temperature-dependent factors are omitted, the model is given by

$$\mu = \mu_{min} + \frac{\mu_{max} - \mu_{min}}{1 + \left(\frac{N_t}{N_{ref}}\right)^{\alpha}}, \tag{16}$$

where N_t is the total doping density, μ_{min}, μ_{max}, N_{ref} and α are material-specific parameters, which can be obtained either experimentally or from Monte Carlo simulations.

The default parameters used in equation (16) were extracted for $Al_{0.2}Ga_{0.8}N$ and $Al_{0.5}Ga_{0.5}N$, and are presented for the reference doping density $N_{ref} = 10^{17}$ cm^{-3} in Table 1. The parameters for $Al_{0.3}Ga_{0.7}N$ are calculated by a linear interpolation between the nearest available respective values.

Table 1. Default parameters in (16) for $N_{ref} = 10^{17}$ cm^{-3}

Material	μ_{min}, $cm^2/(V \cdot s)$	μ_{max}, $cm^2/(V \cdot s)$	α
$Al_{0.2}Ga_{0.8}N$	132.0	306.1	0.29
$Al_{0.5}Ga_{0.5}N$	41.7	208.3	0.12

Phonon-assisted tunneling model. In accordance with the PAT model [8], the current transport through the Schottky barrier is controlled by tunneling from trap centers localized near the metal-semiconductor interface to the conduction band of the semiconductor. Because of continuous charging these centers from the adjacent metal, their occupation density is assumed to be independent of the applied bias. If the electrons emitted from the trap centers dominate the carrier flux through the barrier, the current is evaluated as follows:

$$J_{PAT} = -qWN_s, \tag{17}$$

where W is the rate of PAT of electrons from the trap centers to the conduction band and N_s is the occupied trap center density near the interface.

The rate of PAT as a function of temperature and electric field can be expressed in the form presented in Ref. [13]:

$$W = \frac{\omega}{\beta}\left[(1+\gamma^2)^{\frac{1}{2}} - \gamma\right]^{\frac{1}{2}} (1+\gamma^2)^{-\frac{1}{4}} \exp\left\{-\frac{2\beta E_s}{3\hbar\omega}\left[(1+\gamma^2)^{\frac{1}{2}} - \gamma\right]^2 \left[(1+\gamma^2)^{\frac{1}{2}} + \frac{\gamma}{2}\right]\right\}. \tag{18}$$

Here ω is the frequency of phonon oscillations, E_s is the depth of the occupied trap centers and $\hbar$ is the reduced Planck constant.

In equation (18), β and γ are given by

$$\beta = \frac{2\omega(2m_{eff}m_eE_s)^{\frac{1}{2}}}{q|E|} \tag{19}$$

and

$$\gamma = \frac{\beta\Gamma^2}{16\hbar\omega E_s}. \tag{20}$$

Here Γ is the width of the trap center absorption band. When an electron interacts predominantly with the longitudinal optical phonons, the width depends on temperature as follows:

$$\Gamma^2 = 8\iota\left(\frac{2}{\exp\frac{\hbar\omega}{\kappa T}-1}+1\right)(\hbar\omega)^2, \quad (21)$$

where ι is the electron-phonon interaction constant.

Combined model. In case of the TED model expanded by incorporating the PAT model, the total current is determined by

$$J_S = q\frac{v_D}{v_D+v_R}\left\{v_R n_{eq}\left[\exp\left(-\frac{\varphi_n}{V_T}\right)-1\right]-WN_s\right\}. \quad (22)$$

If WN_s is much less than the minuend in the curly brackets, equation (22) reduces to equation (15) after the quasi-equilibrium concentration of electrons is expressed in accordance with expression (12). In that case, the TED model defines the current and is suitable for describing the forward current-voltage characteristic of the Schottky diode. Otherwise, J_s tends to J_{PAT} from equation (17). Now the current is largely controlled by tunneling from trap centers and the PAT model is suitable for describing the reverse-bias characteristic.

Boundary conditions. After the current density in equation (2) is substituted with the help of equation (22), the system of the Poisson and continuity equations is solved self-consistently to determine the potential and electron concentration profiles. The numerical solution of these coupled non-linear second-order partial differential equations is obtained by the Newton iteration method applied to a linearized version of the complete set of the equations derived by the Scharfetter-Gummel discretization scheme [14].

The self-consistent solutions of the primary equations must simultaneously satisfy the boundary conditions implemented at the diode electrodes.

In case of the rectifying contact, Dirichlet boundary condition is imposed on the Poisson equation, which implies that the surface potential is fixed and defined by

$$\varphi_s = \frac{E_g}{2}+\frac{V_T}{2}\ln\frac{N_c}{N_v}-\varphi_b-\varphi_n, \quad (23)$$

where E_g is the band gap and N_v is the effective density of states in the valence band.

For the continuity equation, the inhomogeneous Neumann condition, when the current through the barrier has to be computed in accordance with the boundary condition (22), is established.

In case of the ohmic contact, Dirichlet boundary conditions are imposed on both semiconductor equations. Assuming charge neutrality and thermal equilibrium along with the validity of Maxwell-Boltzmann statistics, the surface electron concentration can be determined by

$$n_o = \frac{N_d+\sqrt{N_d^2+4n_i^2}}{2}. \quad (24)$$

Here n_i is the intrinsic carrier concentration estimated from material-specific parameters as follows:

$$n_i = \sqrt{N_c N_v}\exp\left(-\frac{E_g}{2V_T}\right). \quad (25)$$

The surface potential at the ohmic contact is defined by

$$\varphi_o = \varphi_n + V_T\ln\frac{n_o}{n_i}. \quad (26)$$

Along the device structure, non-conducting edges, homogeneous Neumann boundary conditions, where the normal component of the electric field becomes zero, are implemented.

Finally, Dirichlet thermal boundary conditions, when the temperature is fixed, are set up around the entire simulation domain, the temperature being constant throughout the whole device structure.

3. Results

The effective density of states in the conduction and valence bands, the electron effective mass and the relative permittivity for $Al_{0.3}Ga_{0.7}N$ are determined through a linear interpolation between the corresponding values for the associated binary materials. The band gap of the ternary compound is calculated as follows:

$$E_g(Al_xGa_{1-x}N) = xE_g(AlN) + (1-x)E_g(GaN) - 1.3x(1-x), \tag{27}$$

where x is the composition fraction.

The electronic band structure and dielectric parameters for $Al_{0.3}Ga_{0.7}N$ are given for convenience in Table 2. The corresponding values for AlN and GaN may be accessed through the references.

Table 2. Electronic band structure and dielectric parameters for $Al_{0.3}Ga_{0.7}N$

Parameter	Value	Unit	References
N_c	$3.5\cdot10^{18}$	cm^{-3}	[15]
N_v	$1.76\cdot10^{20}$	cm^{-3}	[15]
E_g	4.019	eV	[16]
m_{eff}	0.238		[17]
ε	8.78		[15]

The Schottky barrier height in the metal/$Al_{0.3}Ga_{0.7}N$ contact is assigned a value of 1.5 eV, which is derived as the difference between the metal work function and the electron affinity of $Al_{0.3}Ga_{0.7}N$. For the semiconductor layer, a uniform donor density of 10^{17} cm^{-3} is selected. The mobility of electrons computed by equation (16) equals 187.7 $cm^2/(V\cdot s)$. The simulation is performed for a temperature of 300 K. The parameters of the PAT model are taken as typical averaged values from Refs. [8,18,19] and are listed in Table 3.

Table 3. Parameters of the PAT model

Parameter	Value	Unit
N_s	10^{13}	cm^{-2}
ι	1.7	
ω	$1.063\cdot10^{14}$	s^{-1}
E_s	0.8	eV

In Figure 1, two variants of the current-voltage (J/V) characteristic of the $Al_{0.3}Ga_{0.7}N$ Schottky diode under a reverse bias with a width of 0.2 μm are presented on a logarithmic scale, one obtained by the TED model and another by a combination of the TED and PAT models.

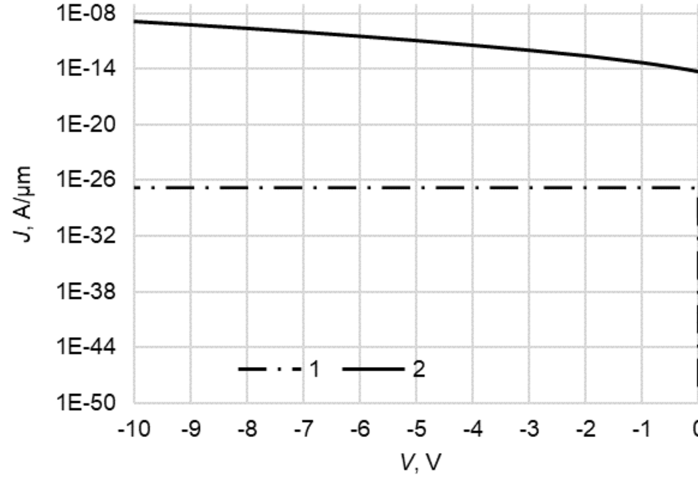

Fig. 1. *J*/*V* characteristic of the $Al_{0.3}Ga_{0.7}N$ Schottky diode with $w = 0.2$ μm described either by the TED model (line 1) or by the combined model (line 2)

It is obvious that, in accordance with the TED model, the current is not flowing (to be more precise, it is tending to zero), when the diode is at the thermal equilibrium, that is, no bias is applied. At the same time, the combined model predicts a certain non-zero value of the current ($J_s = -5.094 \cdot 10^{-15}$ A/μm). Moreover, J_{TED} takes a non-zero value immediately after a reverse bias is applied ($J_{TED} = -4.736 \cdot 10^{-28}$ A/μm at $V = -0.01$ V).

In Figures 2 and 3, the same characteristics are drawn separately on a linear scale. It is not difficult to note that J_{TED} exhibits a very weak dependence on the bias, rising only 3.315 times (from $-4.763 \cdot 10^{-28}$ A/μm to $-1.579 \cdot 10^{-27}$ A/μm), when V is changed from -0.01 V to -10 V. It can be judged from equation (15) that the reverse-bias leakage current generated by thermionic emission, diffusion and drift depends on V primarily through the effective diffusion velocity.

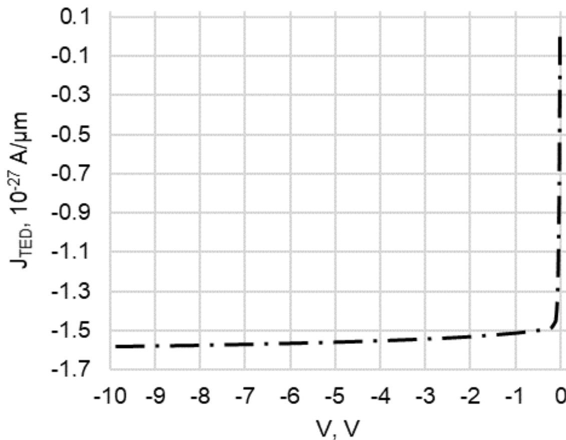

Fig. 2. J_{TED}/*V* characteristic of $Al_{0.3}Ga_{0.7}N$ Schottky diode with $w = 0.2$ μm

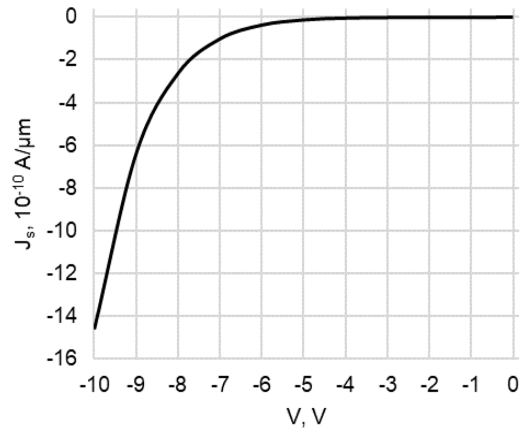

Fig. 3. J_s/*V* characteristic of $Al_{0.3}Ga_{0.7}N$ Schottky diode with $w = 0.2$ μm

In contrast to J_{TED}, J_s appears to be a strong function of V, increasing $2.3 \cdot 10^5$ times (from $-5.094 \cdot 10^{-15}$ A/μm to $-1.461 \cdot 10^{-9}$ A/μm), when the bias is raised from 0 V to -10 V. Analysis of equation (22) shows that since the density of the occupied trap centers near the metal-semiconductor interface is considered to be independent of the bias, J_s and V are coupled mainly through the electric field or the gradient of the electrostatic potential, which

define the center-to-band tunneling rate. The potential, in its turn, is distributed along the device structure in simultaneous accordance with the bias and the distance between the electrodes. It follows from here that the leakage currents of Schottky diodes with identical parameters but featuring varying widths of the structure are expected to be unequal for the same bias conditions.

In Figure 4, the profiles of the electric field constructed on several mesh nodes nearest to the metal-semiconductor interface are drawn for the $Al_{0.3}Ga_{0.7}N$ Schottky diode with different distances between the electrodes. A bias voltage of -10 V is applied. It follows from the simulation results that for identical bias conditions the intensity of the electric field at the metal-semiconductor interface is larger for the diode structure with a lesser width. The intensity rises by 5.5 % (from $-7.764\cdot 10^5$ V/cm to $-8.192\cdot 10^5$ V/cm) when the structure is narrowed from 0.2 μm to 0.18 μm, and 13.1 % (from $-7.764\cdot 10^5$ V/cm to $-8.778\cdot 10^5$ V/cm) in case the width is decreased from 0.2 μm to 0.16 μm.

In Figure 5, three variants of the J_s/V characteristic of the $Al_{0.3}Ga_{0.7}N$ Schottky diode are presented, each obtained for a different width. It is evident that the less the distance between the electrodes the larger the leakage current of the $Al_{0.3}Ga_{0.7}N$ Schottky diode for identical bias conditions, since the electric field defines the probability of electron center-to-band tunneling. At $V = -10$ V, J_s rises 1.9 times (from $-1.461\cdot 10^{-9}$ A/μm to $-2.844\cdot 10^{-9}$ A/μm), when the diode structure is narrowed from 0.2 μm to 0.18 μm, and increases 4.6 times (from $-1.461\cdot 10^{-9}$ A/μm to $-6.681\cdot 10^{-9}$ A/μm) in case the width is lessened from 0.2 μm to 0.16 μm. Concerning the Schottky-barrier AlGaN/GaN HEMT, it means that if the total thickness of the barrier and buffer layers does not exceed the width of the space charge region, the gate leakage current increases, when the epitaxial layers are made thinner, thus, limiting design flexibility.

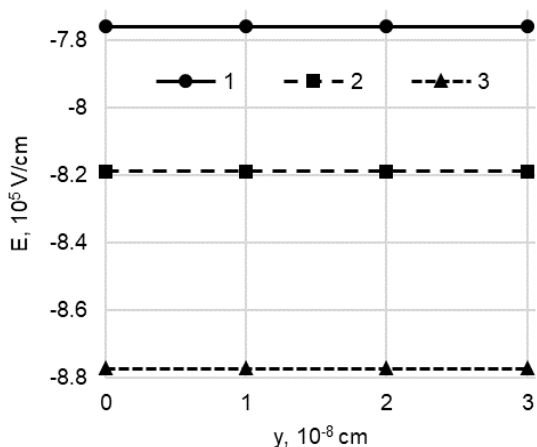

Fig. 4. Profiles of the electric field for $Al_{0.3}Ga_{0.7}N$ Schottky diode with $w = 0.2$ μm (line 1), 0.18 μm (line 2), 0.16 μm (line 3) at $V = -10$ V

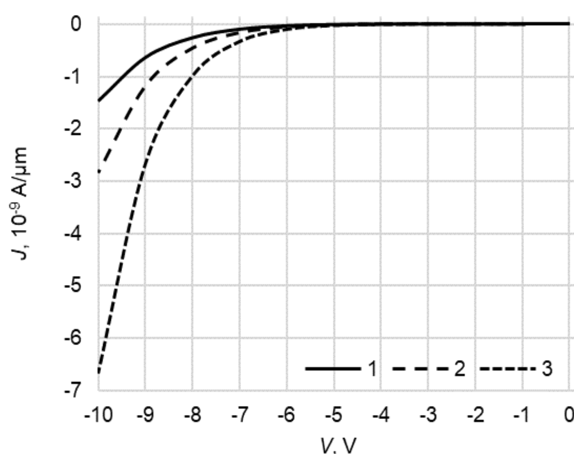

Fig. 5. J_s/V characteristic of $Al_{0.3}Ga_{0.7}N$ Schottky diode with $w = 0.2$ μm (line 1), 0.18 μm (line 2) and 0.16 μm (line 3)

Overall the combined model employed to estimate the leakage current in the AlGaN Schottky contact shows a good agreement with experimental data. In Figure 6, the J/V characteristic of the $Al_{0.3}Ga_{0.7}N$ Schottky diode (w = 1.42 μm) calculated either by the TED model or by the combined model is compared with the input characteristic of the $Al_{0.3}Ga_{0.7}N$/GaN HEMT (the total thickness of the epitaxial structure equals 1.42 μm) obtained experimentally in Ref. [20].

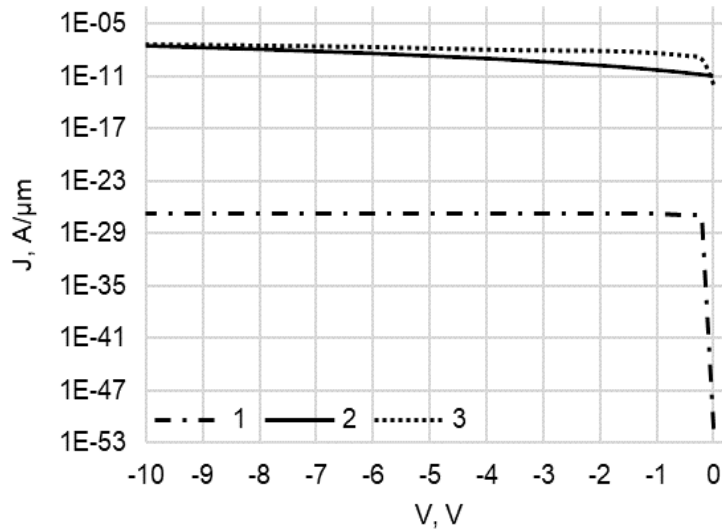

Fig. 6. *J*/*V* characteristic of the $Al_{0.3}Ga_{0.7}N$ Schottky diode (*w* = 1.42 μm) described by the TED (line 1) and the combined (line 2) models in comparison with the input characteristic of the $Al_{0.3}Ga_{0.7}N$/GaN HEMT obtained experimentally (line 3)

Analysis of Figure 6 shows that the combined model provides a much more accurate estimation of the leakage current than the TED theory. Thus, the currents in the Schottky contacts of the diode and the HEMT are predicted to be of the same order, when the applied bias is at least -7 V. The discrepancy observed at low biases is thought to be mainly due to the presence of the heterojunction in the transistor structure.

4. Conclusions

The combination of the TED and the PAT models proves to be efficient in describing the reverse-bias characteristic of the AlGaN Schottky contact. It can serve as a base to develop a more sophisticated model, which would predict accurately the gate leakage current in the AlGaN/GaN HEMT.

Acknowledgments. *This work was supported by the grants 1.8.05 of Belarusian National Scientific Research Program "Informatics, Space, Safety" and 3.2.01 Belarusian National Scientific Research Program "Photonics, Opto- and Microelectronics".*

References

[1] Deen D, Storm D, Meyer D, Scott Katzer D, Bass R, Binari S, Gougousi T. AlN/GaN HEMTs with high-κ ALD HfO_2 or Ta_2O_5 gate insulation. *Physica Status Solidi C*. 2011;8(7-8): 2420-2423.

[2] Chen J, Kawanago T, Wakabayashi H, Tsutsui K, Iwai H, Nohata D, Nohira H, Kakushima K. La_2O_3 gate dielectrics for AlGaN/GaN HEMT. *Microelectronics Reliability*. 2016;60: 16-19.

[3] Miller EJ, Yu ET, Waltereit P, Speck JS. Analysis of reverse-bias leakage current mechanisms in GaN grown by molecular-beam epitaxy. *Applied Physics Letters*. 2004;84(4): 535-537.

[4] Zhang H, Miller EJ, Yu ET. Analysis of leakage current mechanisms in Schottky contacts to GaN and $Al_{0.25}Ga_{0.75}N$/GaN grown by molecular-beam epitaxy. *Journal of Applied. Physics*. 2006;99(2): 023703.

[5] Huang S, Chen B, Wang MJ. Current transport mechanism of AuNiGaN Schottky diodes at high temperatures. *Applied Physics Letters.* 2007;91(7): 072109.

[6] Arslan E, Butun S, Ozbay E. Leakage current by Frenkel-Poole emission in Ni/Au Schottky contacts on $Al_{0.83}In_{0.17}N$/AlN/GaN heterostructures. *Applied Physics Letters.* 2009;94(14): 142106.

[7] Iucolano F, Roccaforte F, Giannazzo F, Raineri V. Influence of high-temperature GaN annealed surface on the electrical properties of Ni/GaN Schottky contacts. *Journal of Applied Physics.* 2008;104(9): 093706.

[8] Pipinys P, Lapeika V. Temperature dependence of reverse-bias leakage current in GaN Schottky diodes as a consequence of phonon-assisted tunneling. *Journal of Applied Physics.* 2006;99(9): 093709.

[9] Wang A, Martin-Horcajo S, Tadjer MJ, Calle F. Simulation of temperature and electric field-dependent barrier traps effects in AlGaN/GaN HEMTs. *Semiconductor Science and Technology.* 2015;30(1): 015010.

[10] Crowell CR, Sze SM. Current transport in metal-semiconductor barriers. *Solid-State Electronics.* 1966;9: 1035-1048.

[11] Schroeder D. *Modeling of Interface Carrier Transport for Device Simulation.* New York: Springer-Verlag; 1994.

[12] Farahmand M, Garetto C, Bellotti E, Brennan KF, Goano M, Ghillino E, Ghione G, Albrecht JD, Ruden PP. Monte Carlo simulation of electron transport in the III-nitride wurtzite phase materials system: binaries and ternaries. *IEEE Transactions on Electron Devices*. 2001;48(3): 535-542.

[13] Kiveris A, Kudzmauskas S, Pipinys P. Release of electrons from traps by an electric field with phonon participation. *Physica Status Solidi A*. 1976;37: 321-327.

[14] Scharfetter DL, Gummel HK. Large signal analysis of a silicon read diode oscillator. *IEEE Transactions on Electron Devices*. 1969;16(1): 64-77.

[15] Levinshtein ME, Rumyantsev SL, Shur MS. *Properties of Advanced Semiconductor Materials: GaN, AlN, InN, BN, SiC, SiGe*. John Wiley & Sons; 2001.

[16] Chuang SL, Chang CS. A band-structure model of strained quantum-well wurtzite semiconductors. *Semiconductor Science and Technology.* 1997;12(3): 252-263.

[17] Kim K, Lambrecht WRL, Segall B, Schilfgaarde M. Effective masses and valence-band splittings in GaN and AlN. *Physical Review B.* 1997;56(12): 7363-7375.

[18] Pipinys P, Pipiniene A, Rimeika A. Phonon-assisted tunneling in reverse biased Schottky diodes. *Journal of Applied Physics*. 1999;86(12): 6875-6878.

[19] Pipinys P, Lapeika V. Analysis of reverse-bias leakage current mechanisms in metal/GaN Schottky diodes. *Advances in Condensed Matter Physics.* 2010;2010(2): 529629.

[20] Mi M, He Y, Hou B, Zhang M, Zhang J, Wang C, Ma X, Hao Y. Threshold voltage engineering in GaN-based HEMT by using La_2O_3 gate dielectric. *Physica Status Solidi C*. 2016;13(5-6): 325-327.